Science Signaling
AAAS

www.sciencesignaling.org/cgi/content/full/2/90/ra59/DC1

Supplementary Materials for

Hippo Pathway–Dependent and –Independent Roles of RASSF6

Mitsunobu Ikeda, Akira Kawata, Misa Nishikawa, Yuko Tateishi, Masato Yamaguchi, Kentaro Nakagawa, Susumu Hirabayashi, Yijun Bao, Shiho Hidaka, Yukio Hirata, Yutaka Hata*

*To whom correspondence should be addressed. E-mail: yuhammch@tmd.ac.jp

Published 29 September 2009, *Sci. Signal.* **2**, ra59 (2009)
DOI: 10.1126/scisignal.2000300

This PDF file includes:

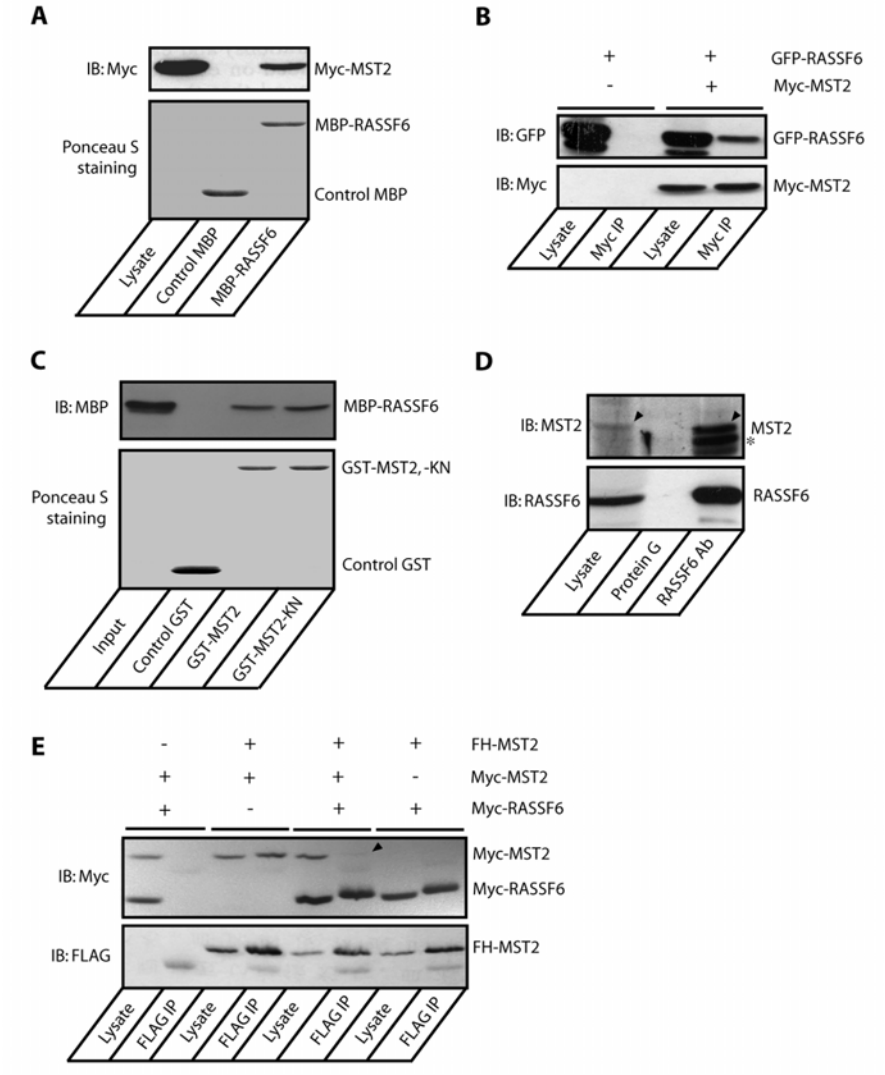

fig. S1. Interaction of RASSF6 with MST2. (**A**) Pull-down assays were performed using lysates of COS-7 cells expressing Myc-MST2 and 250 pmol MBP or MBP-RASSF6 immobilized on 10 μl of amylose resin beads. The samples were immunoblotted with anti-Myc. MBP-RASSF6 captured Myc-MST2. (**B**) GFP-RASSF6 was expressed alone or with Myc-MST2 in COS-7 cells. Immunoprecipitation was performed with anti-Myc. (**C**) 50 pmol of purified MBP-RASSF6 was incubated with 10 pmol GST, GST-MST2 or GST-MST2-kinase negative (KN) immobilized on 10 μl of glutathione-Sepharose beads. 1 μg of MBP-RASSF6 was run as input control (input). (**D**) RASSF6 and MST2 coimmunoprecipitate from rat liver. RASSF6 was immunoprecipitated from lysates prepared from rat hepatocytes (4 x 10^7 cells), and the precipitates were immunoblotted with anti-MST2 and anti-RASSF6. Arrowheads and asterisk indicate MST2 and the immunoglobulin heavy chain, respectively. (**E**) FH-MST2, Myc-MST2, and Myc-RASSF6 were expressed in HEK293 cells. FLAG immunoprecipitates were immunoblotted with anti-Myc and anti-FLAG. Coimmunoprecipitation of Myc-MST2 with FLAG-MST2 was blocked by Myc-RASSF6 (arrowhead).

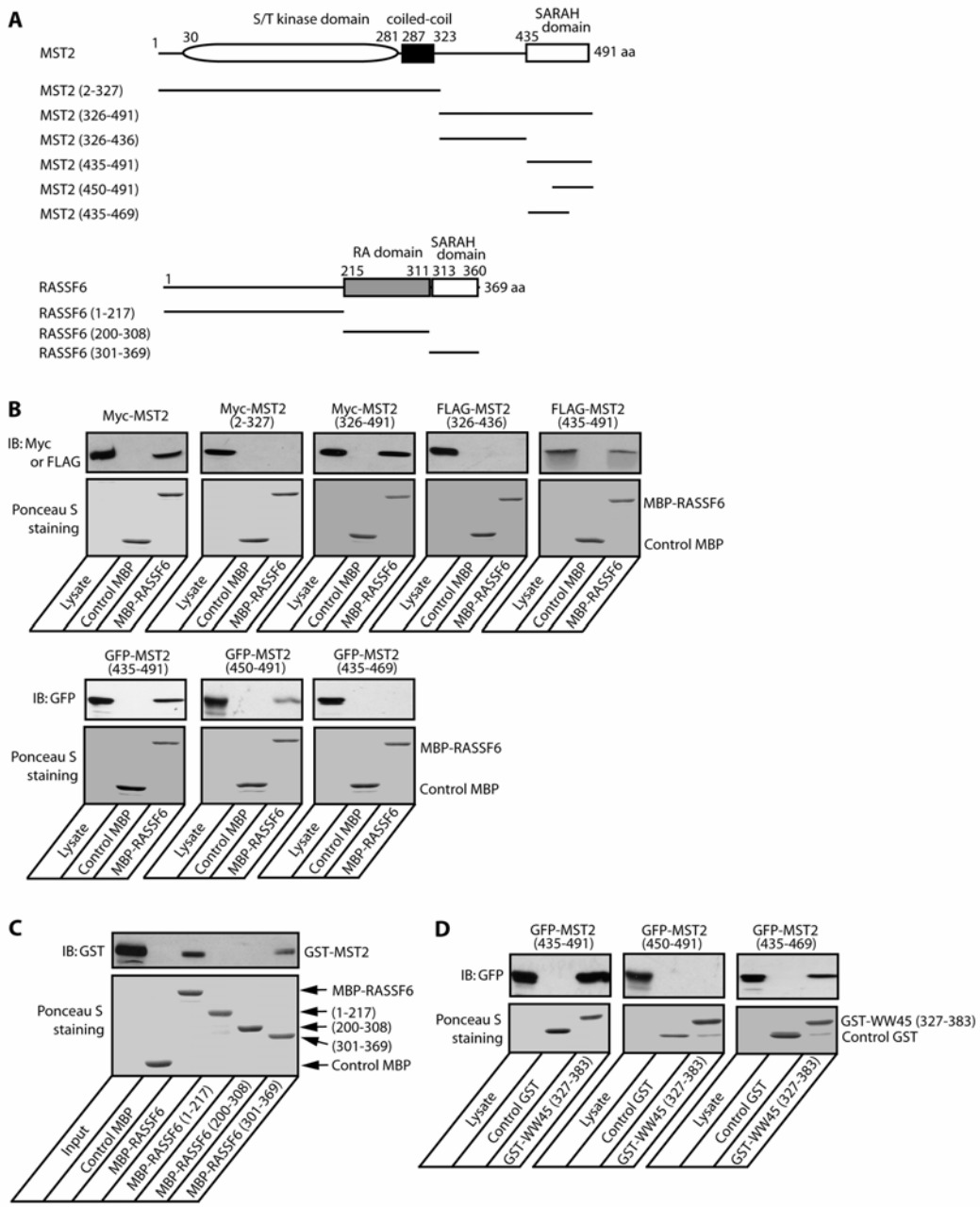

fig. S2. Molecular determinants of the interaction of MST2 with RASSF6 and WW45. (**A**) Schematic representation of various MST2 and RASSF6 constructs. The white oval, black box, white box, and gray box represent the serine/threonine (S/T) kinase domain, coiled-coil region, SARAH domain, and Ras association (RA) domain, respectively. Numbers indicate the first and the last amino acid residues of each domain and each protein. (**B**) Pull-down assays were performed using lysates of COS-7 cells expressing various Myc-, FLAG- and GFP-tagged MST2 proteins with MBP and MBP-RASSF6 immobilized on amylose resin beads. MBP-RASSF6 captured Myc-MST2, Myc-MST2 (326-491), and FLAG-MST (435-491). It also trapped GFP-MST2 (435-491) and GFP-MST2 (450-491). (**C**) Pull-down assays were performed using purified GST-MST2 and various MBP-tagged proteins immobilized on amylose resin beads. (**D**) Pull-down assays were performed using lysates of COS-7 cells expressing various GFP-tagged MST2 proteins with GST or GST-WW45 (327-383). GST-WW45 (327-383) bound GFP-MST2 (435-491) and GFP-MST2 (435-469).

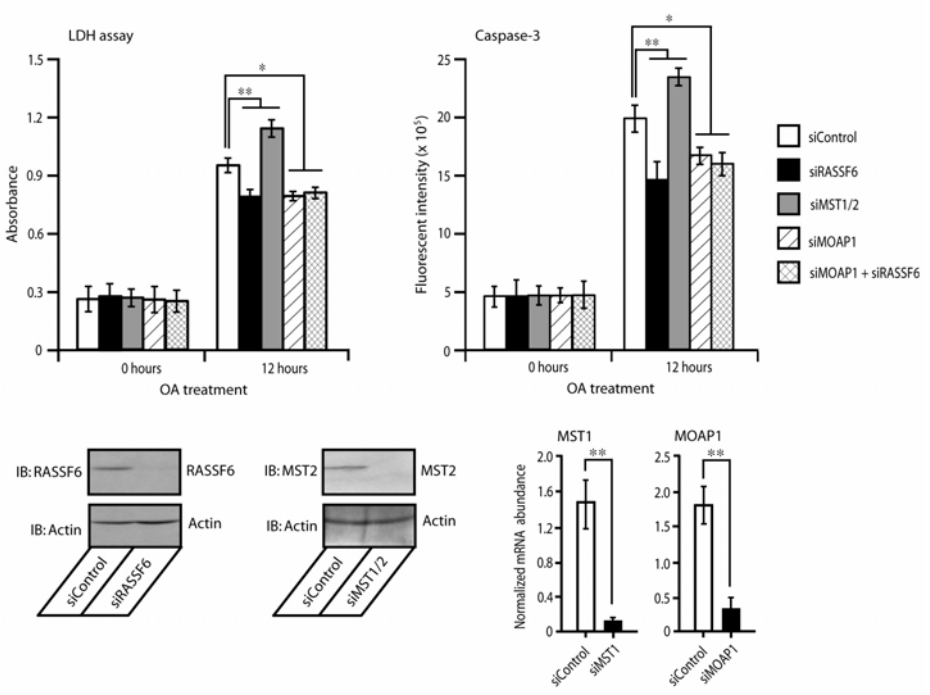

fig. S3. OA treatment induces apoptosis in rat hepatocytes. Knockdown of RASSF6 and MOAP1 partially suppressed LDH release and caspase-3 activation in OA-treated hepatocytes, whereas knockdown of MST1 and MST2 enhanced these measures. Knockdowns were confirmed by immunoblotting for RASSF6 and MST2 and by quantitative RT-PCR for MST1 and MOAP1. * $P < 0.05$; ** $P < 0.01$.

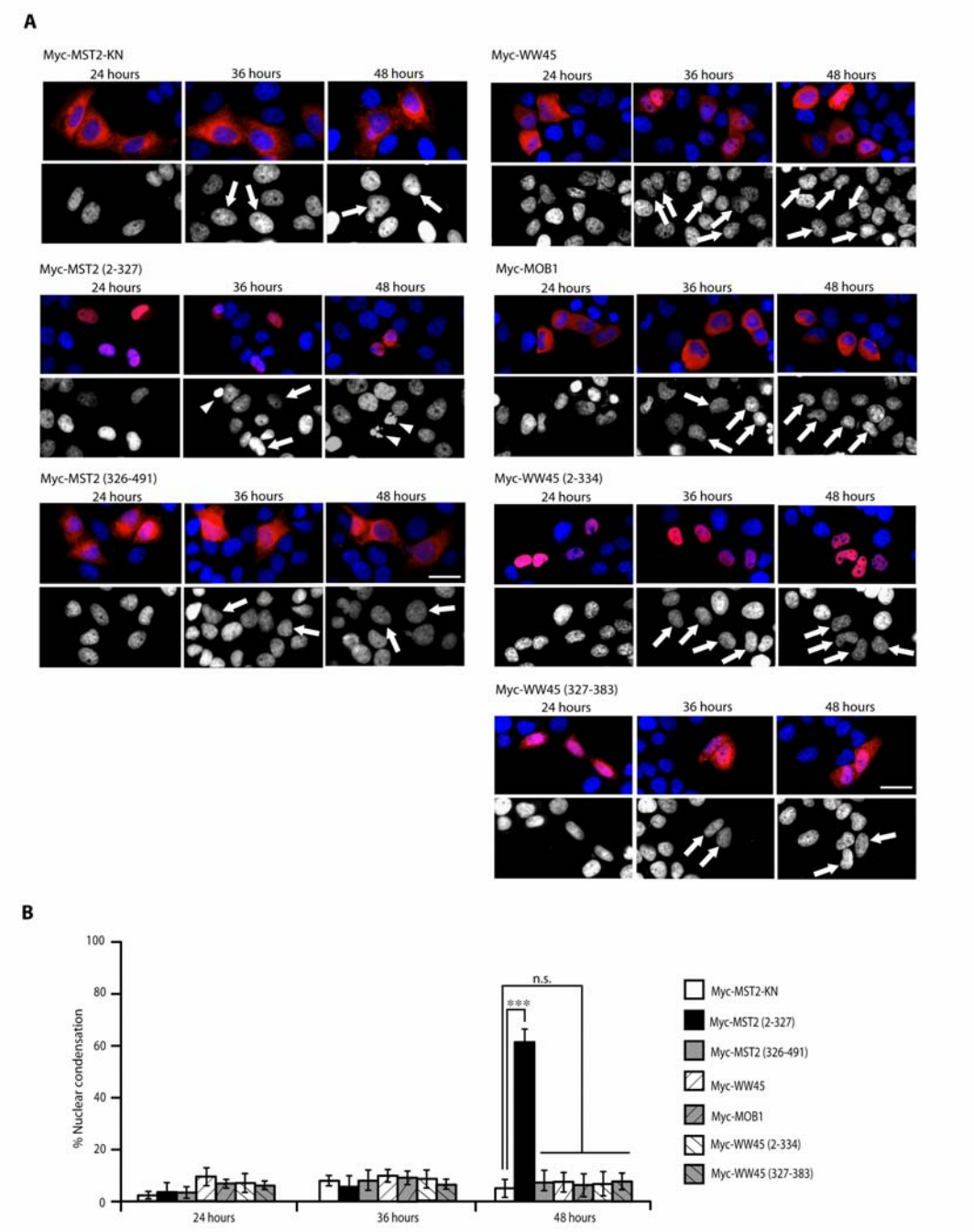

fig. S4. The effect of the expression of various MST2 and WW45 proteins. (**A**) Myc-MST2-KN, Myc-MST2 (2-327), Myc-MST2 (326-491), Myc-WW45, Myc-WW45 (2-334), Myc-WW45 (327-383), or Myc-MOB1 was expressed in HeLa cells. Myc-MST2 (2-327) induced nuclear condensation (arrowheads), but the other constructs did not (arrows). Scale bar, 50 μm. (**B**) Quantification of cells with nuclear condensation. 50 to 100 cells were analyzed for each treatment. Error bars indicate S.D. of three independent experiments. *** $P < 0.001$; n.s., not significant.

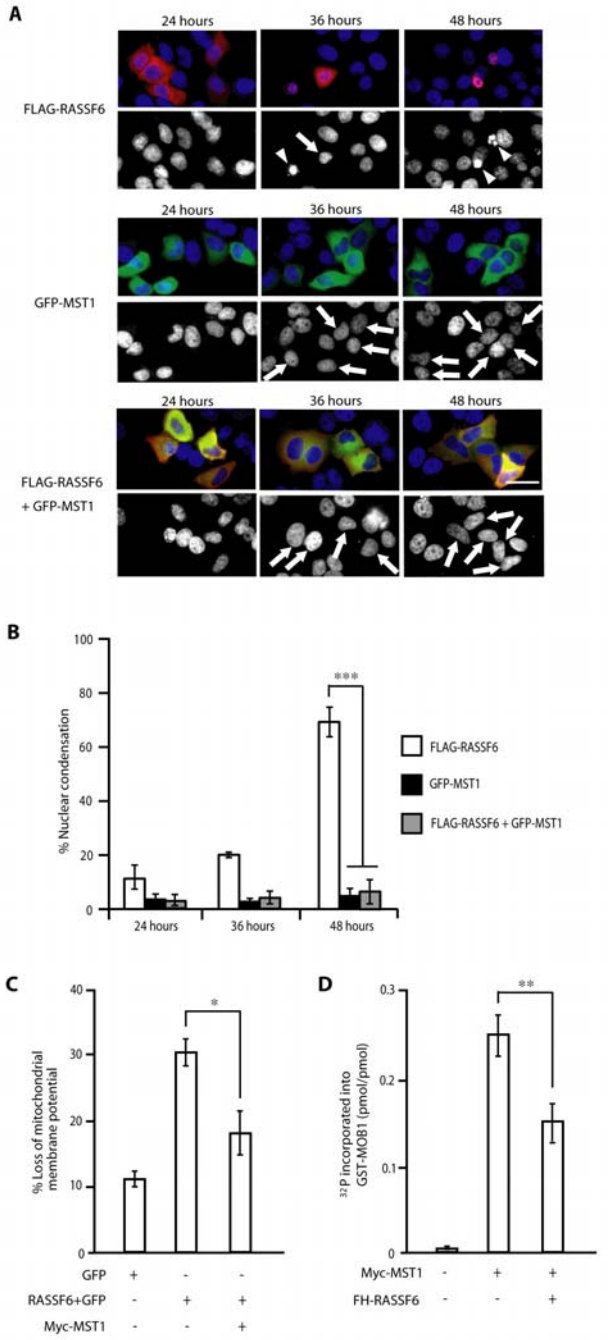

fig. S5. MST1 inhibits RASSF6-induced apoptosis, whereas RASSF6 inhibits the phosphorylation of MOB1 by MST1. (**A**) HeLa cells expressing GFP-MST1 and FLAG-RASS6 were fixed and immunostained with anti-FLAG at the indicated time periods after transfection. Nuclei were visualized with Hoechst 33342. FLAG-RASSF6-expressing cells exhibited nuclear condensation (arrowheads). GFP-MST1 blocked nuclear condensation in FLAG-RASSF6-epxressing cells (arrows). (**B**) Quantification of cells with nuclear condensation was performed as described for fig. S4B. (**C**) HeLa cells expressing GFP, FLAG-RASSF6 and GFP (RASSF6+GFP), and Myc-MST1 were loaded with 200 nM of tetramethylrhodamine methyl ester (TMRM). Mitochondrial membrane permeability was evaluated in GFP-positive cells using FACS. (**D**) Myc-MST1 was expressed alone or with FH-RASSF6 in HEK293 cells, immunoprecipitated, and used to phosphorylate GST-MOB1. * P <0.05; ** P < 0.01; *** P < 0.001.

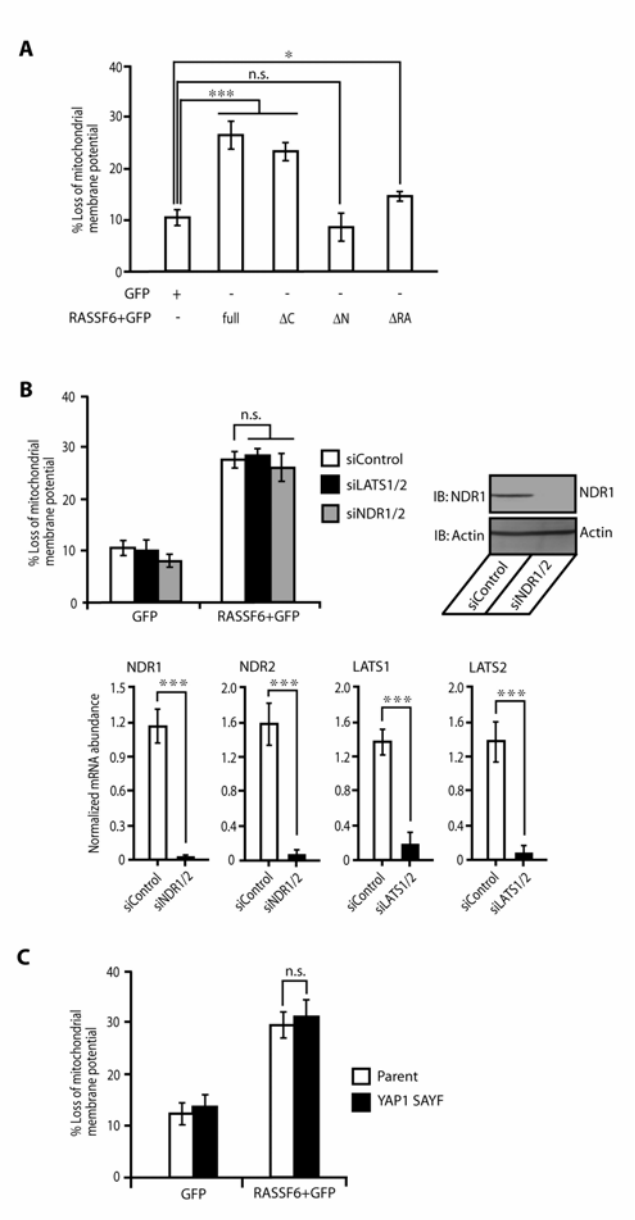

fig. S6. RASSF6-induced apoptosis is independent of the interaction with MST2 and NDR kinases. (**A**) Mitochondrial membrane permeability was evaluated in HeLa cells expressing various RASSF6 proteins using TMRM and FACS. RASSF6 lacking the SARAH domain (ΔC) induced apoptosis, whereas RASSF6 lacking the N-terminal region (ΔN) or the Ras-association domain (ΔRA) did not. (**B**) The effect of knockdown of NDR1 and NDR2 or LATS1 and LATS2 on RASSF6-induced apoptosis. HeLa cells were transfected with siRNAs directed against NDR1 and NDR2 (siNDR1/2) or against LATS1 and LATS2 (siLATS1/2), and with GFP or FLAG-RASSF6 together with GFP (RASSF6+GFP). Mitochondrial membrane permeability was evaluated in GFP-positive cells using TMRM and FACS. Knockdowns were confirmed by quantitative RT-PCR. Suppression of NDR1 at the protein level is also demonstrated. (**C**) The effect of the YAP1 S127A Y407F mutant (YAP1 SAYF) on RASSF6-induced apoptosis. Control GFP or FLAG-RASSF6 together with GFP (RASSF6+GFP) was expressed in parent or YAP1 S127A Y407F-expressing HeLa cells. * $P < 0.05$; *** $P < 0.001$; n.s., not significant.

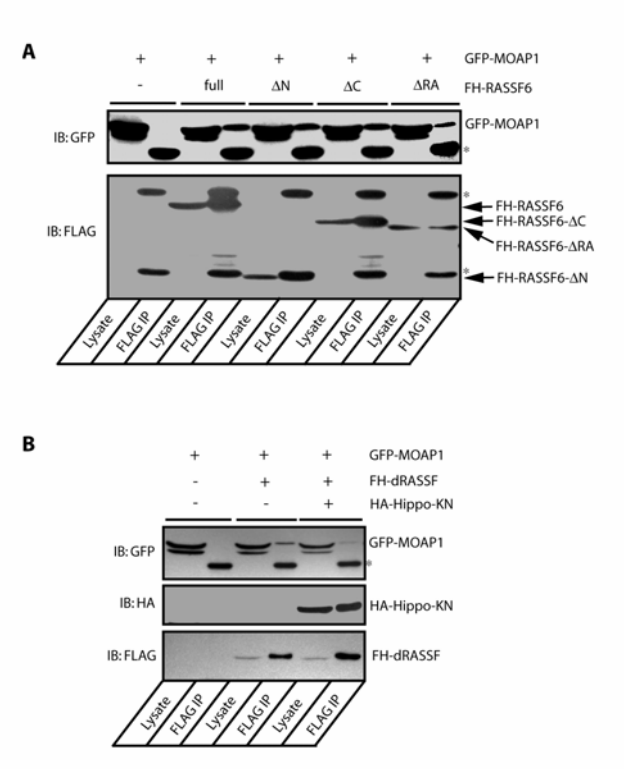

fig. S7. Interaction of MOAP1 with RASSF6 and dRASSF. (**A**) and (**B**) GFP-MOAP1, various FH-RASSF6 proteins, FH-dRASSF, and HA-Hippo-KN were expressed in various combinations in HEK293 cells. FLAG immunoprecipitates were probed with anti-GFP and anti-FLAG. GFP-MOAP1 coimmunoprecipitated with all tested deleted RASSF6 proteins and FH-dRASSF. HA-Hippo-KN blocked the coimmunoprecipitation of GFP-MOAP1 and FH-dRASSF. Asterisks indicate immunoglobulin light and heavy chains.

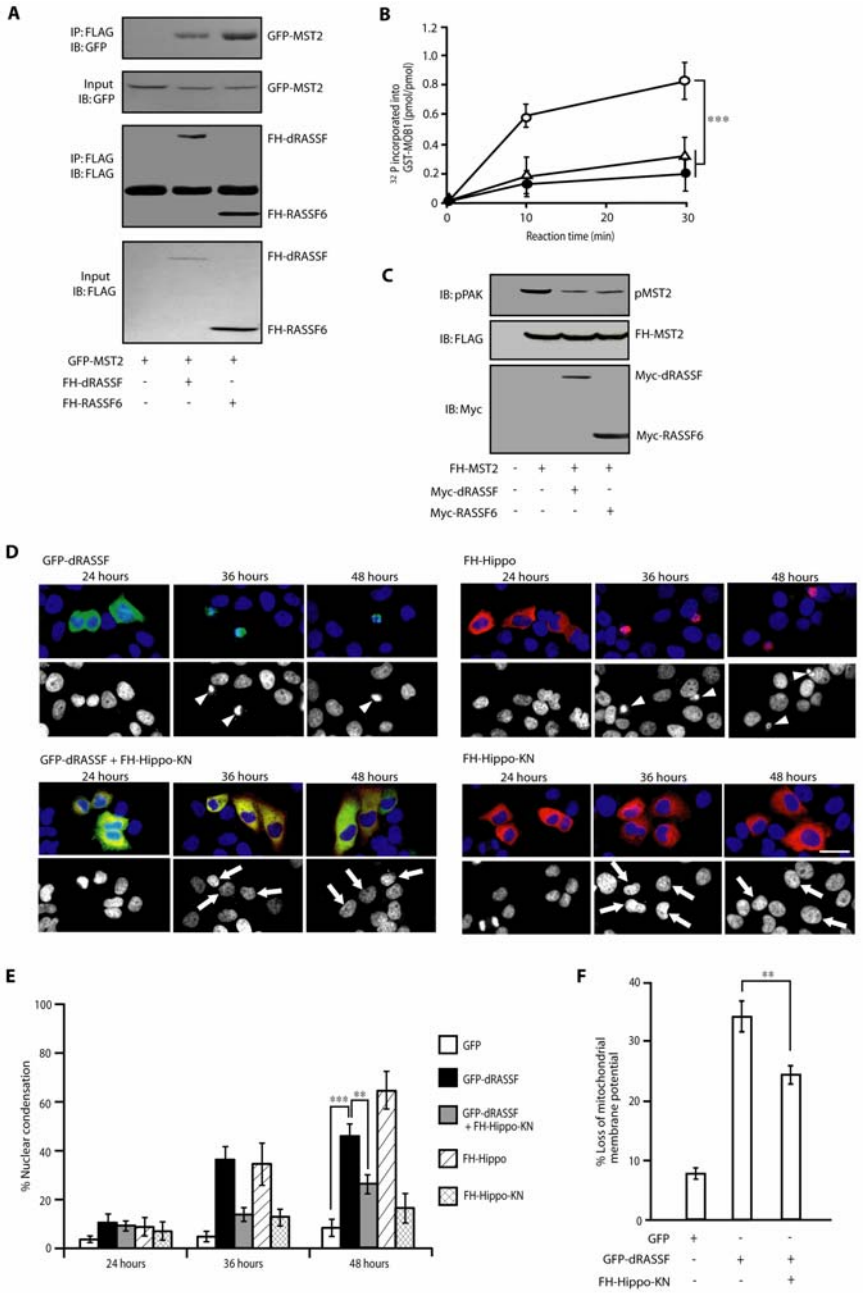

fig. S8. dRASSF interacts with and inhibits MST2. (**A**) Interaction between dRASSF and MST2. GFP-MST2 was expressed alone or with FH-dRASSF or FH-RASSF6 in HEK293 cells. FLAG immunoprecipitates were probed with anti-GFP and anti-FLAG. (**B**) In vitro inhibition of MST2 by dRASSF. FH-MST2 was expressed alone or with Myc-dRASSF or Myc-RASSF6 in HEK293 cells, immunoprecipitated with anti-FLAG, eluted with FLAG peptide, and used to phosphorylate GST-MOB1. MST2 alone (open circles); MST2 and dRASSF (open triangles); and MST2 with RASSF6 (closed circles). (**C**) Inhibition of MST2 by dRASSF. FH-MST2 was expressed alone or with Myc-dRASSF or Myc-RASSF6 in HEK293 cells and probed with anti-phospho-PAK1, anti-FLAG, and anti-Myc. (**D**) dRASSF-induced apoptosis in HeLa cells. GFP-dRASSF and FH-Hippo caused nuclear condensation in HeLa cells (arrowheads), whereas FH-Hippo-KN did not (arrows). FH-Hippo-KN inhibits nuclear condensation in GFP-dRASSF-expressing HeLa cells (arrows). Scale bar, 50 μm. (**E**) Quantification of cells with nuclear condensation was performed as described for fig. S4B. (**F**) Mitochondrial membrane permeability was evaluated as described for fig. S5C. ** $P < 0.01$; *** $P < 0.001$.

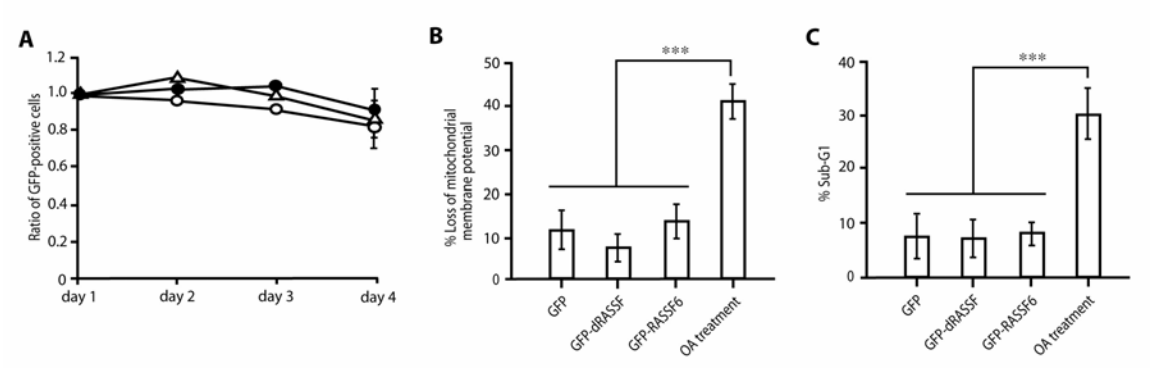

fig. S9. dRASSF or RASSF6 does not induce apoptosis in S2 cells. (**A**) Control GFP (open circles), GFP-dRASSF (closed circles), or GFP-RASSF6 (open triangles) were expressed in S2 cells. The number of GFP-positive cells was counted using FACS at the indicated time points. S2 cells expressing GFP-dRASSF or GFP-RASSF6 remained viable. (**B**) Mitochondrial membrane permeability was evaluated as described for fig. S5C. (**C**) DNA content of GFP-positive cells was evaluated using propidium iodide and FACS. ***P<0.001.

Table S1. Twenty-one–nucleotide oligomers used in this study

Target Gene	Sense	Antisense
Human WW45	5’-gcccuucuuacagaguuggtt-3’	5’-ccaacucuguaagaagggctt-3’
Rat RASSF6	5’-uucgaugaccuuuaccguatt-3’	5’-uacgguaaaggucaucgaatt-3’
Human MST1 Stealth	5’-aaugauaucagauacagaaccagcc-3’	5’-ggcugguucuguaucugauaucauu-3’
Rat MST1	5’-cgauauuauucggcuccgatt-3’	5’-ucggagccgaauaauaucgga-3’
Human MST2 Stealth	5’-uuuccugaagaucugauucaacagg-3’	5’- ccuguugaaucagaucuucaggaaa -3’
Rat MST2	5’-gacauaauuagauuacgaatt-3’	5’-uucguaaucuaauuauguctg-3’
Human NDR1	5’-ggccuaaaagaugaggagatt-3’	5’-ucuccucaucuuuuaggcctt-3’
Human NDR2	5’-ggauuagcagaugaagagatt-3’	5’-ucucuucaucugcuaaucctt-3’
Human LATS1	5’-acuuugccgaggacccgaatt-3’	5’-uucggguccucggcaaagutt-3’
Human LATS2	5’-ggaccaaacagugacacuutt-3’	5’-aagugucacuguuuggucctg-3’
Human MOAP1	5’-ggcgauugcuagagagccutt-3’	5’-aggcucucuagcaaucgcctt-3’
Rat MOAP1	5’-ggucagauaccuuacuacutt-3’	5’-aguaguaagguaucugacctg-3’

Table S2. Primers for quantitative RT-PCR

Target Gene	Sense	Antisense
Rat MST1	5’-aagagctggactgtggagga-3’	5’-gtgctggctaacagacacga-3’
Human NDR1	5’-atttggtgaggtacggcttg-3’	5’-caggcaggaactccatgatt-3’
Human NDR2	5’-ctcacacacaacccaccaag-3’	5’-cactcccaaagaccaccagt-3’
Human LATS1	5’-gtccttcgtgtgggctacat-3’	5’-cgaggatcttcggttgacat-3’
Human LATS2	5’-ttcatccaccgagacatcaa-3’	5’-ctccatgctgtcctgtctga-3’
Human MOAP1	5’-cagtgggtgagttgagcaga-3’	5’-gaaacatccagcgtccaaat-3’
Rat MOAP1	5’-taggggagcacagactgctt-3’	5’-tcattccgattcccaagaac-3’
Human actin	5’-cccagcaccatgaagatcaagatc-3’	5’-cctgcttggtgatccacatctgc-3’
Rat actin	5’-agccatgtacgtagccatcc-3’	5’-ctctcagctgtggtggtgaa-3’